Title

p75 neurotrophin receptor regulates tissue fibrosis through inhibition of plasminogen activation via a PDE4/cAMP/PKA pathway

Permalink

https://escholarship.org/uc/item/4xm667p6

Journal

Journal of Cell Biology, 177(6)

ISSN

0021-9525

Authors

Sachs, Benjamin D
Baillie, George S
McCall, Julianne R
et al.

Publication Date

2007-06-18

DOI

10.1083/jcb.200701040

Peer reviewed

p75 neurotrophin receptor regulates tissue fibrosis through inhibition of plasminogen activation via a PDE4/cAMP/PKA pathway

Benjamin D. Sachs,[1] George S. Baillie,[2] Julianne R. McCall,[1] Melissa A. Passino,[1] Christian Schachtrup,[1] Derek A. Wallace,[2] Allan J. Dunlop,[2] Kirsty F. MacKenzie,[2] Enno Klussmann,[3] Martin J. Lynch,[2] Shoana L. Sikorski,[1] Tal Nuriel,[1,4] Igor Tsigelny,[1] Jin Zhang,[1] Miles D. Houslay,[2] Moses V. Chao,[4] and Katerina Akassoglou[1]

[1]Department of Pharmacology, University of California, San Diego, La Jolla, CA 92093
[2]Molecular Pharmacology Group, Biochemistry & Molecular Biology, University of Glasgow, Glasgow G12 8QQ, Scotland, UK
[3]Leibniz-Institut für Molekulare Pharmakologie (FMP), Campus Berlin-Buch, 13125 Berlin, Germany
[4]Molecular Neurobiology Program, Skirball Institute of Biomolecular Medicine, Departments of Cell Biology, Physiology, and Neuroscience, New York University School of Medicine, New York, NY 10016

Clearance of fibrin through proteolytic degradation is a critical step of matrix remodeling that contributes to tissue repair in a variety of pathological conditions, such as stroke, atherosclerosis, and pulmonary disease. However, the molecular mechanisms that regulate fibrin deposition are not known. Here, we report that the p75 neurotrophin receptor (p75[NTR]), a TNF receptor superfamily member up-regulated after tissue injury, blocks fibrinolysis by down-regulating the serine protease, tissue plasminogen activator (tPA), and up-regulating plasminogen activator inhibitor-1 (PAI-1).

We have discovered a new mechanism in which phosphodiesterase PDE4A4/5 interacts with p75[NTR] to enhance cAMP degradation. The p75[NTR]-dependent down-regulation of cAMP results in a decrease in extracellular proteolytic activity. This mechanism is supported in vivo in p75[NTR]-deficient mice, which show increased proteolysis after sciatic nerve injury and lung fibrosis. Our results reveal a novel pathogenic mechanism by which p75[NTR] regulates degradation of cAMP and perpetuates scar formation after injury.

Introduction

Tissue scarring, characterized by cell activation, excessive deposition of ECM, and extravascular fibrin deposition, is considered a limiting factor for tissue repair. Fibrin, the major substrate of the serine protease plasmin, is a provisional matrix deposited after vascular injury (Bugge et al., 1996). The two plasminogen activators (PAs), namely tissue plasminogen

activator (tPA) and urokinase plasminogen activator (uPA) and their inhibitors, such as plasminogen activator inhibitor-1 (PAI-1), are key modulators of scar resolution by spatially and temporally regulating the conversion of plasminogen to plasmin resulting in fibrin degradation and ECM remodeling (Lijnen, 2001). In the peripheral nervous system, previous work by us and others showed that inhibition of fibrinolysis in mice deficient in plasminogen or tPA exacerbated axonal damage (Akassoglou et al., 2000) and impaired functional recovery after nerve injury (Siconolfi and Seeds, 2001). In accordance, mice deficient for fibrinogen showed increased regenerative capacity (Akassoglou et al., 2002). Studies of fibrin deposition in human diseases, in combination with experiments from mice deficient in plasminogen and PAs, have provided information about a wide range of physiological and pathological conditions that are exacerbated by defective fibrin degradation, such as wound healing, metastasis, atherosclerosis, lung ischemia, rheumatoid arthritis, muscle regeneration, and multiple sclerosis (MS) (Degen et al., 2001; Adams et al., 2004).

However, the molecular mechanisms that regulate proteolytic activity remain unclear.

In our current work, we focus on the mechanisms that regulate fibrinolysis after injury. Our previous studies demonstrated a correlation between fibrin deposition and expression of p75 neurotrophin receptor (p75[NTR]) after nerve injury (Akassoglou et al., 2002). Up-regulation of p75[NTR] is observed in MS (Dowling et al., 1999), stroke (Park et al., 2000), and spinal cord (Beattie et al., 2002) and sciatic nerve injury (Taniuchi et al., 1986), all of which are associated with fibrin deposition. p75[NTR] is also expressed in non-neuronal tissues (Lomen-Hoerth and Shooter, 1995) and is up-regulated in non-nervous system diseases associated with defects in fibrin degradation, such as atherosclerosis (Wang et al., 2000), melanoma formation (Herrmann et al., 1993), lung inflammation (Renz et al., 2004), and liver disease (Passino et al., 2007). p75[NTR] has been primarily characterized as a modulator of cell death (Wang et al., 2000) and differentiation (Passino et al., 2007) in non-neuronal tissues. The expression of p75[NTR] by cell types such as smooth muscle cells and hepatic stellate cells, which actively participate in tissue repair by migration, and secretion of ECM and extracellular proteases, raises the possibility for a functional role of p75[NTR] in disease pathogenesis that extends beyond apoptosis and differentiation.

We find that p75[NTR] is involved in the regulation of proteolytic activity and fibrin degradation. Mice deficient for p75[NTR] (Lee et al., 1992) show increased proteolytic activity and decreased fibrin deposition in two disease models: sciatic nerve injury and lung fibrosis. p75[NTR] regulates proteolytic activity by simultaneously down-regulating tPA and up-regulating PAI-1 via a novel cAMP/PKA pathway. p75[NTR] decreases cAMP via interaction with the cAMP-specific phosphodiesterase (PDE) isoform PDE4A4/5. This is of particular note, as selective PDE4 inhibitors have an anti-inflammatory action and have potential therapeutic utility in inflammatory lung disease, as well as in a wide range of neurologic diseases such as depression, spinal cord injury, MS, and stroke (Gretarsdottir et al., 2003; Nikulina et al., 2004; Houslay et al., 2005). Overall, the regulation of plasminogen activation by p75[NTR] identifies a novel pathogenic mechanism whereby p75[NTR] interacts with PDE4A4/5 to degrade cAMP and thus perpetuates scar formation that could possibly render the environment hostile for tissue repair.
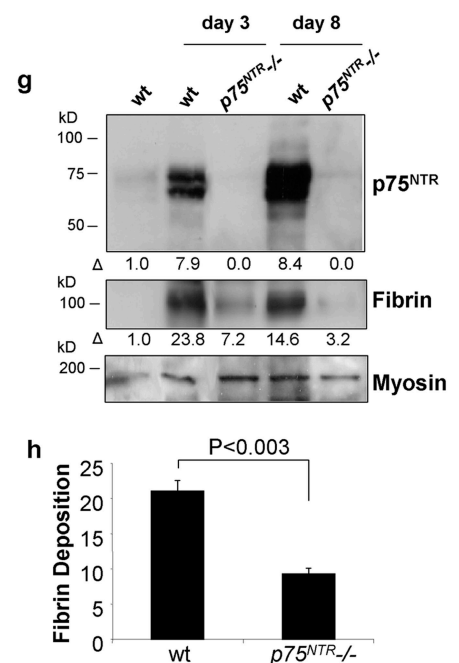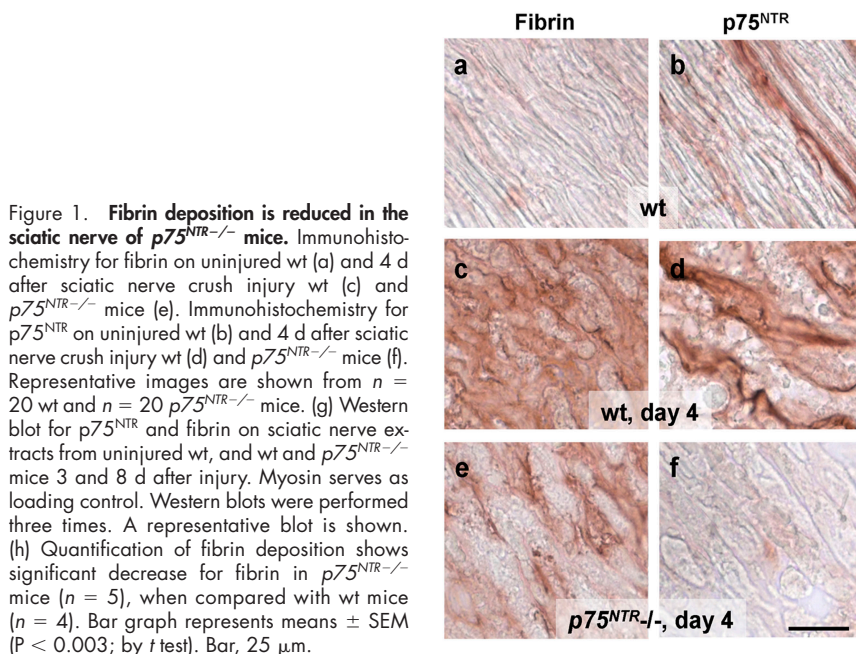
Results

Fibrin deposition is reduced in *p75[NTR−/−]* mice

To examine whether p75[NTR] regulates fibrin deposition in the sciatic nerve we compared fibrin levels in wild-type (wt) and *p75[NTR−/−]* mice after injury. In wt mice, there is a dramatic increase of fibrin deposition (Fig. 1 c) and p75[NTR] expression (Fig. 1 d) after injury, when compared with uninjured nerves (Fig. 1, a and b). In contrast, *p75[NTR−/−]* mice show reduced fibrin deposition after injury (Fig. 1 e). Quantification of immunoblots reveals that *p75[NTR−/−]* mice have decreased fibrin by threefold 3 d and fourfold 8 d after injury (Fig. 1 g). Quantification of fibrin immunostaining also reveals that *p75[NTR−/−]* mice have significantly decreased fibrin (Fig. 1 h, P < 0.003). These results suggest that loss of p75[NTR] decreases the levels of fibrin in the sciatic nerve after injury.

p75[NTR] regulates expression of tPA in the sciatic nerve after crush injury

Analysis of total fibrinogen levels were similar in the plasma of wt and *p75[NTR−/−]* mice (unpublished data), suggesting the decrease in fibrin deposition is not the result of hypofibrinogenemia. Because fibrin removal depends on proteolytic activity (Bugge et al., 1996), we hypothesized that the decreased fibrin in the *p75[NTR−/−]* mice reflects an up-regulation of the proteolytic activity. *p75[NTR−/−]* mice have increased proteolytic activity (Fig. 2 b)

Figure 1. **Fibrin deposition is reduced in the sciatic nerve of *p75[NTR−/−]* mice.** Immunohistochemistry for fibrin on uninjured wt (a) and 4 d after sciatic nerve crush injury wt (c) and *p75[NTR−/−]* mice (e). Immunohistochemistry for p75[NTR] on uninjured wt (b) and 4 d after sciatic nerve crush injury wt (d) and *p75[NTR−/−]* mice (f). Representative images are shown from *n* = 20 wt and *n* = 20 *p75[NTR−/−]* mice. (g) Western blot for p75[NTR] and fibrin on sciatic nerve extracts from uninjured wt, and wt and *p75[NTR−/−]* mice 3 and 8 d after injury. Myosin serves as loading control. Western blots were performed three times. A representative blot is shown. (h) Quantification of fibrin deposition shows significant decrease for fibrin in *p75[NTR−/−]* mice (*n* = 5), when compared with wt mice (*n* = 4). Bar graph represents means ± SEM (P < 0.003; by *t* test). Bar, 25 μm.

when compared with wt mice (Fig. 2 a) that is statistically significant (Fig. 3 i, P < 0.05). Uninjured nerves exhibit minimal proteolytic activity (Fig. 2 i), as expected (Akassoglou et al., 2000). Injured $p75^{NTR-/-}$ sciatic nerves do not show lysis of fibrin in the absence of plasminogen (Fig. 2 c), suggesting that the proteolytic activity is plasminogen dependent.

The tPA/plasmin system regulates fibrin clearance after nerve injury (Akassoglou et al., 2000). A specific tPA inhibitor, tPASTOP, blocks proteolytic activity in $p75^{NTR-/-}$ mice (Fig. 2 d). $p75^{NTR}$ is strongly activated by withdrawal of axons (Lemke and Chao, 1988) and its expression correlates with proliferating, non-myelin producing Schwann cells (SCs) (Zorick and Lemke, 1996). After sciatic nerve injury both $p75^{NTR}$ (Fig. 2 e, red) and tPA (Fig. 2 e, green) increase when compared with uninjured controls (Fig. 2 j), but show little colocalization (Fig. 2, e and h), suggesting that $p75^{NTR}$-reexpressing SCs do not express tPA. Expression of tPA (Fig. 2 k, red) and $p75^{NTR}$ (Fig. 2 l, red) in SCs is confirmed using double immunofluorescence with the SC marker S100 (Fig. 2, k and l; green).

Genetic loss of tPA rescues the effects of p75^NTR deficiency

To examine genetically whether the increased proteolytic activity in the $p75^{NTR-/-}$ mice was due to tPA, we crossed $p75^{NTR-/-}$ mice with $tPA^{-/-}$ mice and generated $p75^{NTR-/-}tPA^{-/-}$ double-knockout mice. $p75^{NTR-/-}$ mice show a decrease in fibrin deposition (Fig. 3 b) and an increase in proteolytic activity (Fig. 3 f), compared with wt control mice (Fig. 3, a and e, respectively). In contrast, $p75^{NTR-/-}tPA^{-/-}$ mice show increased fibrin deposition (Fig. 3 c) when compared with $p75^{NTR-/-}$ mice (Fig. 3 b)

and no evidence of proteolytic activity (Fig. 3 g). As a control, $tPA^{-/-}$ mice also show no evidence of proteolytic activity after sciatic nerve crush injury (Fig. 3 h), as described previously (Akassoglou et al., 2000). Quantification of proteolytic activity is shown in Fig. 3 i. The evidence derived from the genetic depletion of tPA in the $p75^{NTR-/-}$ mice ($p75^{NTR-/-}tPA^{-/-}$ mice, Fig. 3 g) are in accordance with the pharmacologic inhibition of tPA activity in the $p75^{NTR-/-}$ sciatic nerve using tPASTOP (Fig. 2 d). Overall, these results suggest that up-regulation of proteolytic activity in the sciatic nerve of $p75^{NTR-/-}$ mice is due to up-regulation of tPA.

p75^NTR-/- SCs show increased expression of tPA and increased fibrinolysis

Because SCs are a major source for tPA after injury, we isolated primary SCs from wt and $p75^{NTR-/-}$ mice and cultured them on a three-dimensional (3D) fibrin gel. Wt SCs, which express high levels of $p75^{NTR}$, form a monolayer on the fibrin gel (Fig. 4 a). In contrast, $p75^{NTR-/-}$ SCs degrade the fibrin gel (Fig. 4 b) and show a 2.7-fold increase of fibrin degradation (Fig. 4 c). $p75^{NTR-/-}$ SCs show a sixfold increase in tPA levels, when compared with wt SCs (Fig. 4 d; P < 0.01). These results suggest that $p75^{NTR}$ down-regulates tPA activity and blocks fibrin degradation in SCs in vitro.

Expression of p75^NTR inhibits tPA and fibrinolysis

After finding a biological function for $p75^{NTR}$ in the regulation of tPA using SCs and sciatic nerves from $p75^{NTR-/-}$ mice, we used stable and transient transfections of $p75^{NTR}$ as well as
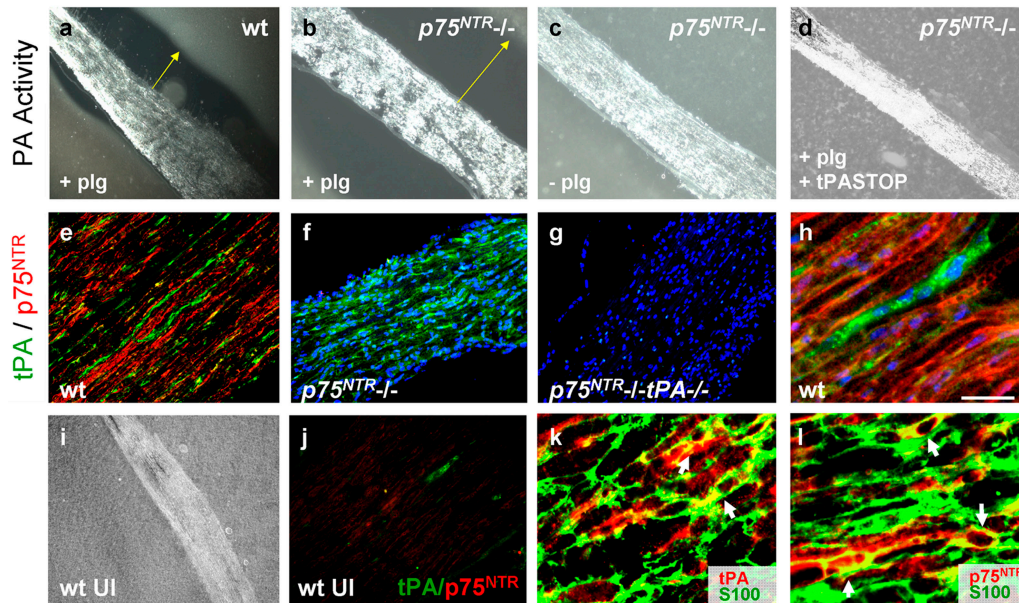

Figure 2. **p75^NTR regulates expression of tPA in the sciatic nerve after crush injury.** In situ zymography in the presence of plasminogen on wt (a) and $p75^{NTR-/-}$ (b) mice and in the absence of plasminogen (c) or in the presence of plasminogen and tPASTOP (d) in $p75^{NTR-/-}$ mice. Arrows indicate the lytic zone. Double immunofluorescence for tPA (green) or $p75^{NTR}$ (red) on wt (e and h), $p75^{NTR-/-}$ (f) and $p75^{NTR-/-}tPA^{-/-}$ mice (g). Uninjured wt sciatic nerve exhibits minimal proteolytic activity (i) and minimal tPA and $p75^{NTR}$ immunoreactivity (j). Zymographies have been performed on n = 10 wt and n = 10 $p75^{NTR-/-}$ mice. Representative images are shown. tPA (k) and $p75^{NTR}$ (l) expression in SCs was verified by double immunofluorescence with an S100 (SC marker) antibody. Arrows indicate double-positive cells (k and l, yellow). The experiment was repeated at two different time points (4 and 8 d after crush injury) in n = 4 mice per genotype per time point and representative images are shown. Bar: 400 μm (a–d, i), 150 μm (e–g, j), 20 μm (h, k, and l).
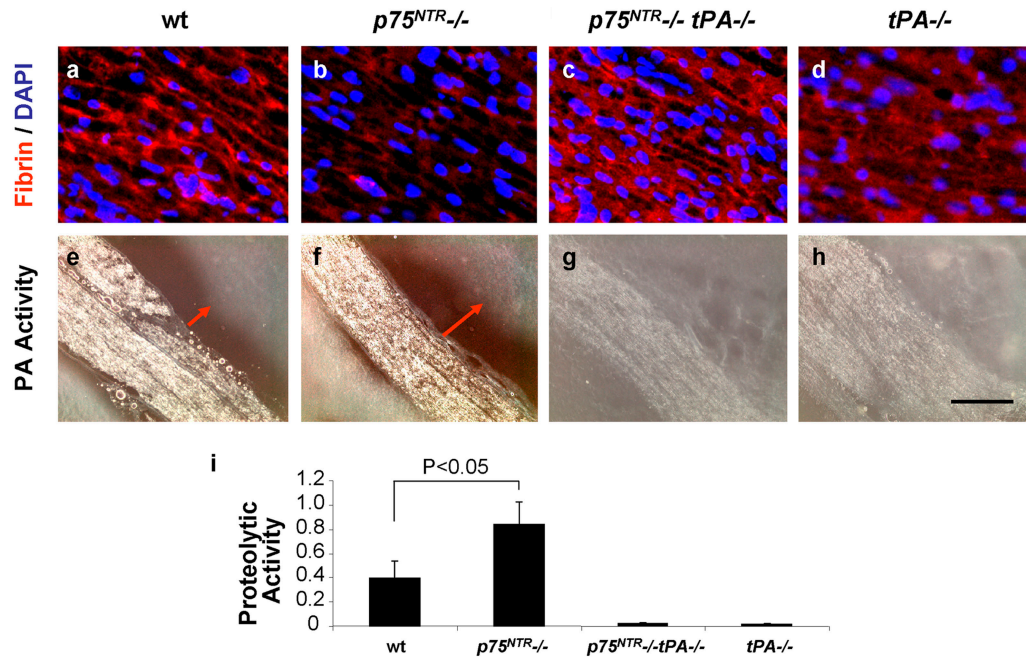
Figure 3. **Loss of tPA rescues the effects of p75^{NTR} deficiency in plasminogen activation and fibrin deposition in the sciatic nerve.** Increased fibrin deposition in the crushed sciatic nerve of *p75$^{NTR-/-}$tPA$^{-/-}$* mice (c), when compared with crushed *p75$^{NTR-/-}$* sciatic nerve (b). Wt (a) and *tPA$^{-/-}$* (d) nerves are used for control. In situ zymography shows lack of proteolytic activity in the crushed *p75$^{NTR-/-}$tPA$^{-/-}$* sciatic nerves (*n* = 5) (g), when compared with crushed *p75$^{NTR-/-}$* sciatic nerves (*n* = 20) (f). Crushed wt (e) and *tPA$^{-/-}$* (h) nerves are used for control. Fibrin immunostainings and zymographies were performed on *n* = 5 *p75$^{NTR-/-}$tPA$^{-/-}$*, *n* = 20 *p75$^{NTR-/-}$*, *n* = 20 wt, *n* = 5 *tPA$^{-/-}$* mice. Representative images are shown. (i) Quantification of proteolytic activity 4 d after crush injury shows statistically significant increase for proteolytic activity in *p75$^{NTR-/-}$* mice. Quantification results are based on *n* = 5 *p75$^{NTR-/-}$*, *n* = 5 *p75$^{NTR-/-}$* *tPA$^{-/-}$*, *n* = 5 *tPA$^{-/-}$* and *n* = 4 wt mice. Bar graph represents means ± SEM (*, P < 0.05; by ANOVA). Bar: 50 μm (a–d), 300 μm (e–h).

siRNA against *p75^{NTR}* to test the properties of p75^{NTR} in heterologous systems. To examine whether p75^{NTR} could inhibit fibrin degradation, we first used NIH3T3 fibroblasts stably transfected with p75^{NTR} that exhibit high levels of p75^{NTR} (10^5 receptors/cell) (Hsu and Chao, 1993). NIH3T3 cells on a 3D fibrin gel degrade fibrin (Fig. 5 a), whereas NIH3T3p75^{NTR} cells do not (Fig. 5 b). Expression of p75^{NTR} inhibits fibrin degradation by 12-fold (Fig. 5 c; P < 0.001). NIH3T3 cells form lytic areas (Fig. 5 d), whereas NIH3T3p75^{NTR} cells grow uniformly on fibrin (Fig. 5 e). NIH3T3 cells fully degrade the plasmin substrate casein (Fig. 5 f) but NIH3T3p75^{NTR} cells do not degrade casein (Fig. 5 g), suggesting impaired proteolysis in NIH3T3p75^{NTR} cells. Aprotinin, a general inhibitor of serine proteases, completely inhibits fibrin degradation by NIH3T3 cells (not depicted). In fibroblasts both tPA and uPA are involved in activation of plasminogen and fibrin degradation. tPA activity is significantly decreased in the NIH3T3p75^{NTR} cells (Fig. 5 h). In contrast, expression of p75^{NTR} has no effect on uPA activity (Fig. 5 i).

tPA is a transcriptionally regulated immediate-early gene (Qian et al., 1993). Indeed, expression of p75^{NTR} down-regulates tPA transcripts (Fig. 5 j). In addition, mRNA of PAI-1 is also up-regulated in NIH3T3p75^{NTR} cells (Fig. 5 j). Real-time quantitative PCR shows a 10.1-fold decrease in tPA mRNA, a fourfold increase in PAI-1 mRNA, and a twofold decrease in uPA mRNA in NIH3T3p75^{NTR} cells. Upon expression of p75^{NTR}, the decrease of uPA RNA does not affect uPA activity (Fig. 5 i). In contrast, the decrease of tPA RNA in NIH3T3p75^{NTR} cells results in a corresponding decrease in tPA activity (Fig. 5 h; P < 0.01).
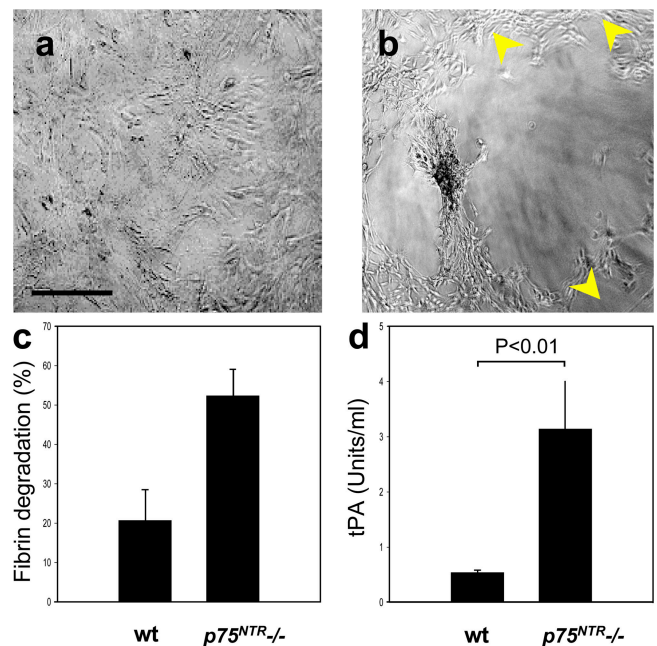

Figure 4. **p75^{NTR}-mediated regulation of tPA and fibrinolysis in SCs.** Primary SC cultures from wt (a) or *p75$^{NTR-/-}$* mice (b) on a 3D fibrin gel. Arrowheads indicate the border of fibrin degradation. Quantification of fibrin degradation (c) and tPA activity (d) from wt and *p75$^{NTR-/-}$* SCs. Experiments were performed three times in duplicates. Representative images are shown. Bar graph represents means ± SEM (P < 0.01; by *t* test). Bar, 130 μm.
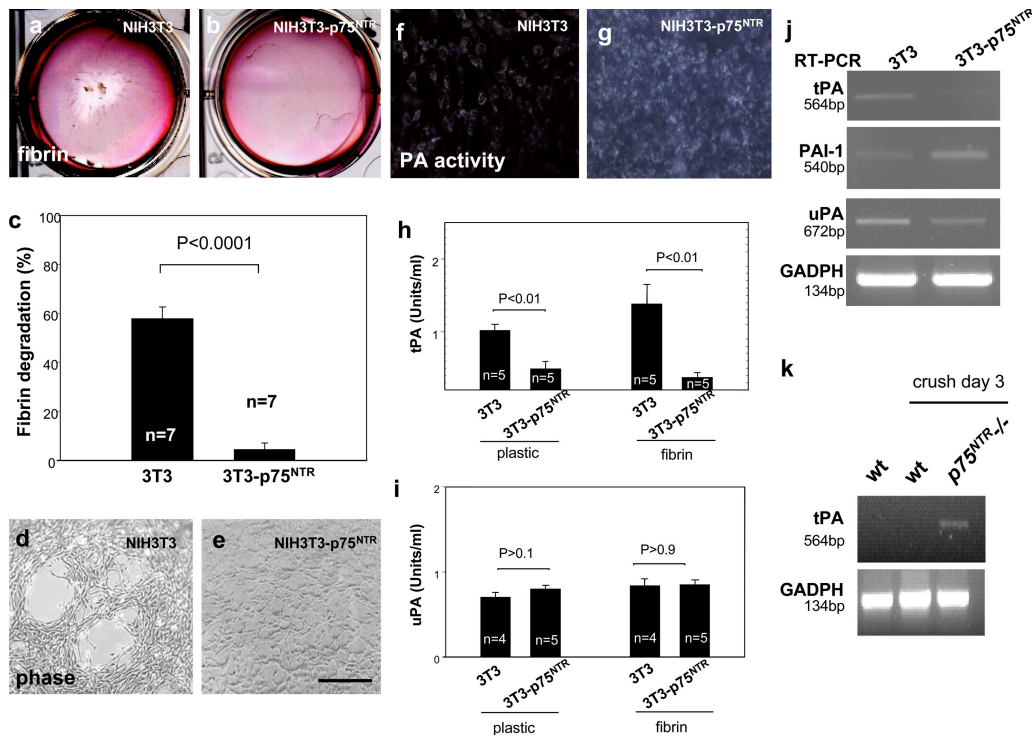
Figure 5. **Expression of p75^NTR regulates tPA, PAI-1, and fibrinolysis in fibroblasts.** 3D fibrin gel degraded by NIH3T3 (a), but not by NIH3T3p75^NTR cells (b). (c) Quantification of fibrin degradation. Experiments were performed seven times in duplicates. Phase-contrast microscopy shows lytic zones in NIH3T3 (d), but not in NIH3T3p75^NTR cultures (e). Zymography shows degradation of casein by NIH3T3 cells (f), whereas NIH3T3p75^NTR cells do not degrade casein (g). Quantification of tPA (h) and uPA (i) activity in supernatants from NIH3T3 and NIH3T3p75^NTR cultures. Experiments were performed five times in duplicates. (j) RT-PCR analysis for *tPA, PAI-1, uPA,* and *GAPDH* on cDNA derived from NIH3T3 and NIH3T3p75^NTR cells. (k) RT-PCR analysis for *tPA* and *GAPDH* on cDNA derived from uninjured wt, and wt or *p75^NTR−/−* mice three days after nerve injury. Bar graphs represent means ± SEM (statistics by *t* test). Bar: 1.2 cm (a and b), 130 μm (d–g).

After injury, sciatic nerves of *p75^NTR−/−* mice show a fourfold increase of *tPA* RNA when compared with wt (Fig. 5 k). Moreover, *p75^NTR−/−* mice show an increase in tPA RNA in primary cerebellar granule neurons (CGNs) (Fig. S1 c, available at http://www.jcb.org/cgi/content/full/jcb.200701040/DC1), and increased proteolytic activity in the cerebellum (Fig. S1, a and b). Overall, these data suggest that expression of p75^NTR inhibits the tPA/plasmin system both in vivo in the cerebellum and after sciatic nerve injury, as well as in vitro in primary neurons, SCs, as well as fibroblasts.

p75^NTR regulates tPA and PAI-1 via a PDE4/cAMP/PKA pathway

Transcriptional regulation of tPA depends on the cAMP/PKA pathway (Medcalf et al., 1990). Indeed, elevation of cAMP, using dibutyryl-cAMP (db-cAMP), overcomes the inhibitory effect of p75^NTR (Fig. 6 a). Moreover, cAMP elevation, elicited using the general PDE inhibitor IBMX, elevates tPA activity in NIH3T3p75^NTR to the levels seen in NIH3T3 cells (Fig. 6 b). IBMX does not affect basal levels of tPA in NIH3T3 cells (Fig. 6 b). These data suggest that PDE activity is required for the p75^NTR-induced tPA decrease.

PKA activity is decreased in NIH3T3p75^NTR cells (Fig. 6 c, lanes 3 and 4) compared with NIH3T3 cells (Fig. 6 c, lanes 1 and 2), suggesting that p75^NTR expression reduces PKA activity. KT5720, a specific PKA inhibitor, decreases tPA activity in

NIH3T3 cells (Fig. 6 b). Because the cAMP/PKA pathway enhances tPA transcription and suppresses PAI-1 secretion (Santell and Levin, 1988), we tested whether the cAMP/PKA pathway influences the p75^NTR regulation of tPA and PAI-1. Forskolin-induced cAMP elevation increases, whereas KT5720-induced PKA inhibition decreases tPA RNA in NIH3T3 cells (Fig. 6 d). Forskolin treatment of NIH3T3p75^NTR cells also increases both tPA RNA (Fig. 6 d) and activity (not depicted), whereas forskolin decreases PAI-1 RNA in both NIH3T3 and NIH3T3p75^NTR cells (Fig. 6 e).

Similar to NIH3T3 cells, elevation of cAMP increases the activity of tPA in both wt and *p75^NTR−/−* SCs (Fig. 6 f). Brain-derived neurotrophic factor (BDNF)/TrkB signaling has been shown to regulate tPA in primary cortical neurons (Fiumelli et al., 1999). In contrast to cortical neurons, SCs are known to express minute levels of TrkB but high levels of p75^NTR (Cosgaya et al., 2002). We show here that treatment of SCs with either BDNF or nerve growth factor (NGF) has no effect on tPA (Fig. 6 f). Similar results are obtained after treatment of SCs with pro-NGF, the high-affinity ligand of p75^NTR (Lee et al., 2001) (unpublished data). In addition, in NIH3T3 and NIH3T3p75^NTR cells, which do not express Trk receptors, the p75^NTR-mediated suppression of tPA activity occurs independent of neurotrophins or serum (unpublished data). In accordance, in NIH3T3 cells transient expression of the intracellular domain (ICD) of p75^NTR decreases tPA similar to the full-length (FL) p75^NTR (Fig. 6 g).
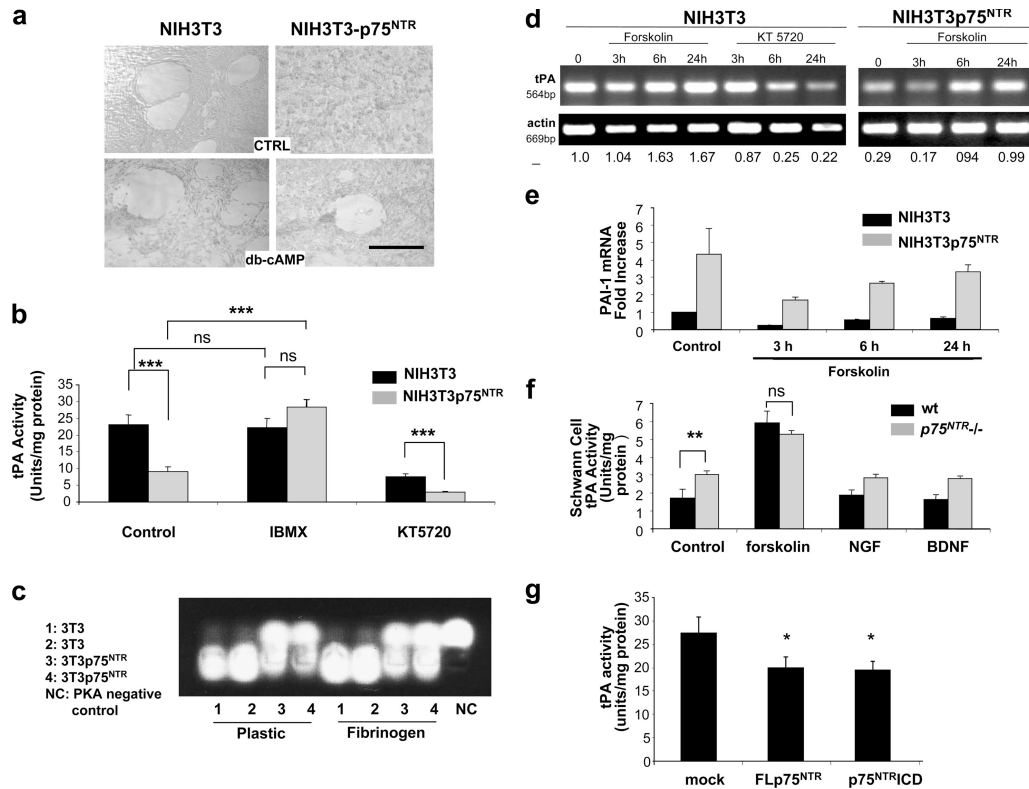
Figure 6. **p75^NTR regulates tPA and PAI-1 via a PDE4/cAMP/PKA pathway.** (a) db-cAMP induces fibrinolysis in NIH3T3p75^NTR cells. (b) IBMX increases tPA activity of NIH3T3p75^NTR cells to the levels of NIH3T3 cells. Inhibition of PKA by KT5720 shows decrease of tPA activity in both NIH3T3 and NIH3T3p75^NTR cells (P < 0.0001). (c) PKA activity assay shows decrease of PKA in NIH3T3p75^NTR cells. (d) Forskolin increases *tPA* mRNA in NIH3T3 and NIH3T3p75^NTR cells. Inhibition of PKA by KT5720 decreases tPA transcript. (e) Quantification of PAI-1 mRNA changes by real time PCR shows a fourfold increase of PAI-1 mRNA in NIH3T3p75^NTR cells compared with NIH3T3 cells. (f) Forskolin increases tPA activity in both wt (P<0.001) and *p75^{NTR−/−}* (P < 0.00001) SCs. NGF and BDNF do not affect activity of tPA (P > 0.8 and P > 0.3, respectively). (g) Transient overexpression of FL p75^NTR or p75 ICD leads to decreased levels of tPA in NIH3T3 cells. Experiments were performed at least 5 times in duplicates. *, P < 0.0001; **, P < 0.05; ***, P < 0.01. NS: non-significant. Bar graphs represent means ± SEM (statistics by ANOVA).

These data suggest that neurotrophin/p75^NTR signaling is not involved in the regulation of tPA in SCs and fibroblasts and that regulation of tPA by p75^NTR is independent of neurotrophins.

p75^NTR decreases cAMP via PDE4

Because the effects of p75^NTR were overcome by elevating cAMP, we examined whether p75^NTR reduced cAMP levels. Indeed, cAMP is decreased 7.8-fold in NIH3T3p75^NTR cells (Fig. 7 a; P < 0.0001). Transient expression of p75^NTR in NIH3T3 cells decreases levels of cAMP (Fig. 7 b; P < 0.0005). Furthermore, siRNA knockdown against *p75^NTR* leads to increased cAMP levels in both NIH3T3p75^NTR cells (Fig. 7, c and e; P < 0.02) and primary SCs (Fig. 7, d and f; P < 0.03). NIH3T3 cells transiently transfected with p75^NTR express five-fold less p75^NTR than the stably transfected NIH3T3p75^NTR cells (unpublished data). Differences in expression between stably and transiently transfected cells may account for the differences in the fold-decrease of cAMP and tPA between these two systems. Moreover, immunostaining with an antibody against cAMP shows increased cAMP in injured sciatic nerves from *p75^{NTR−/−}* mice (Fig. 7, g and h). In neurons BDNF elevates cAMP exclusively via TrkB (Gao et al., 2003). In NIH3T3p75^NTR cells, which do not express TrkB, stimulation with NGF or BDNF does not affect the p75^NTR-mediated suppression of

cAMP (Fig. S2). Similarly, inhibition of neurotrophins by Fc-p75^NTR or BDNF by Fc-TrkB does not alter cAMP levels in NIH3T3p75^NTR cells (Fig. S2, available at http://www.jcb.org/cgi/content/full/jcb.200701040/DC1). In accordance, transient expression of the ICD of p75^NTR decreases cAMP similar to the FL p75^NTR in NIH3T3 cells (Fig. 7 b). Overall, these data suggest a neurotrophin-independent PDE4/cAMP pathway downstream of p75^NTR, which consequently leads to decreases in extracellular proteolysis.

Down-regulation of cAMP can be mediated either by inhibition of cAMP synthesis via the action of G_i, a G protein that inhibits adenylyl cyclase or via the action of PDEs. Treatment of cells with pertussis toxin (PTX) that blocks interactions between the G_i and G protein coupled receptors, does not rescue the p75^NTR-mediated down-regulation of cAMP (Fig. 7 a; P > 0.5). In contrast, the PDE inhibitor IBMX resulted in significant increase of cAMP in the NIH3T3p75^NTR cells when compared with control NIH3T3p75^NTR cells (Fig. 7 a; P < 0.000001). Use of specific chemical inhibitors for PDE isoforms shows that only rolipram, a specific inhibitor of PDE4, significantly increases cAMP levels in NIH3T3p75^NTR cells (Fig. 7 a; P < 0.000001) to the levels of NIH3T3 cells (Fig. 7 a; P = 0.051), suggesting that the p75^NTR-induced cAMP decrease is mediated via PDE4.
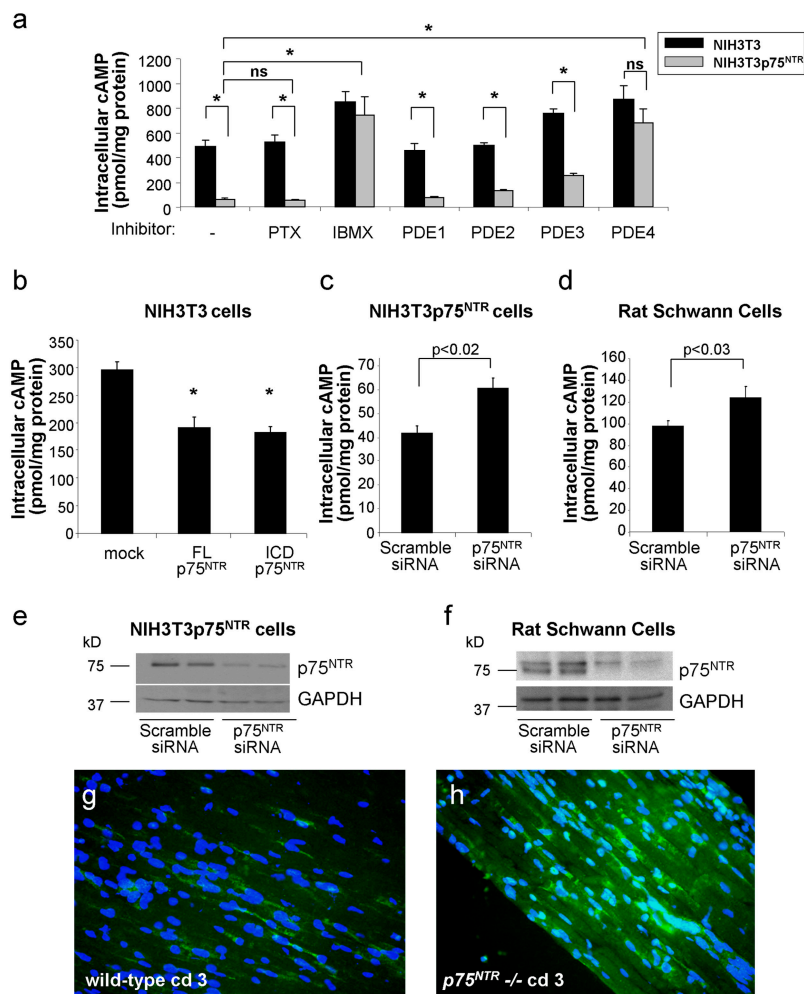
Figure 7. p75^{NTR} decreases intracellular cAMP via PDE4. (a) cAMP levels in NIH3T3 and NIH3T3p75^{NTR} cells show a reduction of cAMP in NIH3T3p75^{NTR} cells, as compared with NIH3T3 cells. Treatment with PTX, IBMX, specific inhibitors for PDE1, PDE2, PDE3, and PDE4 (rolipram) shows that only IBMX (IC50 for PDE4 2–50 μM) and rolipram (IC50 for PDE4 0.8 μM) (P < 0.0001) increase levels of cAMP in NIH3T3p75^{NTR} cells to the levels of NIH3T3 cells. (b) Transient overexpression of FL p75^{NTR} or p75 ICD leads to decreased levels of cAMP in NIH3T3 cells. (c) siRNA mediated knockdown of p75^{NTR} levels in NIH3T3p75^{NTR} cells leads to increased levels of cAMP. (d) siRNA mediated knockdown of p75^{NTR} in primary rat Schwann cells leads to increased levels of cAMP. p75^{NTR} levels after siRNA knock down in duplicate samples of NIH3T3p75^{NTR} cells (e) and SCs (f). Immunostaining to detect cAMP in injured sciatic nerve reveals increased cAMP immunoreactivity in the sciatic nerve of $p75^{NTR-/-}$ mice (h) when compared with wt controls (g). Experiments were performed four times in duplicate. Bar graphs represent means ± SEM (statistics by ANOVA or t test).

p75^{NTR} interacts with PDE4A4/5 and targets cAMP degradation to the membrane

Recruitment of PDE4 to subcellular structures such as the plasma membrane concentrates the activity of PDEs and reduces PKA activity by enhancing degradation of cAMP (Brunton, 2003; Houslay and Adams, 2003). We therefore examined whether p75^{NTR} regulates cAMP via recruitment of PDE4. In NIH3T3p75^{NTR} cells, p75^{NTR} coimmunoprecipitates (co-IPs) with endogenous PDE4A (Fig. 8 a). No association is observed with the other three PDE4 sub-families, namely PDE4B, PDE4C, or PDE4D (unpublished data), suggesting that the effect was PDE4A specific. Based on the molecular weight of PDE4A at 109 kD, we determined that p75^{NTR} co-IPs with the PDE4A5 isoform. Endogenous co-IP in CGNs (Fig. S3 a, available at http://www.jcb.org/cgi/content/full/jcb.200701040/DC1) and in injured sciatic nerve (Fig S3 b) shows that p75^{NTR} and PDE4A5 interact at endogenous expression levels. Analysis of lysates shows that the levels of PDE4A are similar in NIH3T3 and NIH3T3p75^{NTR} cells (Fig. S3 c). These results show that p75^{NTR} forms a complex with PDE4A5.

A functional consequence of the p75^{NTR}–PDE4A5 interaction would be recruitment of PDE4A5 to the membrane resulting in decreased membrane-associated cAMP/PKA signaling.

To investigate whether p75^{NTR} reduces membrane-associated PKA activity, we modified the genetically encoded A-kinase activity reporter, AKAR2 (Zhang et al., 2005) and generated pm-AKAR2.2, a membrane-targeted fluorescent reporter of PKA activity that generates a change in fluorescence resonance energy transfer (FRET) when it is phosphorylated by PKA in living cells (Fig. S4 a). As expected, NIH3T3 cells show a dramatic emission ratio change for the pm-AKAR2.2 in response to forskolin (Fig. 8 b). In contrast, NIH3T3p75^{NTR} cells show an attenuated response, revealing reduced PKA activity at the plasma membrane (Fig. 8 b). Transient transfection of p75^{NTR} confirmed the results observed in the stable NIH3T3p75^{NTR} cells using the latest generation of plasma membrane–specific PKA biosensor AKAR3 (Allen and Zhang, 2006) (Fig. S4 b, available at http://www.jcb.org/cgi/content/full/jcb.200701040/DC1). As expected, increased cAMP degradation at the plasma membrane results in decreased intracellular cAMP (Fig. S4 c; Fig. 7, a and b). Overall, our results showing reduced membrane-associated PKA activity upon expression of p75^{NTR} suggest that p75^{NTR} targets cAMP degradation to the membrane via its interaction with PDE4A5.

To verify the specificity of p75^{NTR}–PDE4A5 association, a series of mapping studies were conducted using deletion mutants. PDE4A5 interacts with FL p75^{NTR}, as well as deletions Δ3, Δ62,

Figure 8. **p75^NTR interacts with PDE4A4/5.** (a) Endogenous PDE4A5 co-IPs with p75^NTR in NIH3T3p75^NTR cells. Lysates were immunoprecipitated with anti-p75^NTR and probed with anti-PDE4A or anti-p75^NTR. Due to the low endogenous levels of PDE4A, higher exposure was necessary to detect PDE4A5 in the lysates (see Fig. S3 c). (b) FRET emission ratio change of NIH3T3 and NIH3T3p75^NTR cells for the pm-AKAR2.2 in response to forskolin. FRET change represents membrane activation of PKA (c) Mapping of the p75^NTR sites required for interaction with PDE4A5. Schematic diagram of HA-tagged p75^NTR intracellular deletions. TM, transmembrane domain; DD, death domain. Lysates were immunoprecipitated with an anti-HA antibody and probed with anti-PDE4A or anti-p75^NTR. (d) Mapping of the PDE4A4 sites required for interaction with p75^NTR. Schematic diagram of the C-terminal deletion of PDE4A4. Arrow indicates the deletion site. Lysates were immunoprecipitated with anti-p75^NTR and probed with anti-PDE4A or anti-p75^NTR. (e) Co-IP of purified, recombinant proteins reveals that both PDE4A4 and PDE4A5 interact with the ICD of p75^NTR, but PDE4D3 does not. (f) PDE4A4 peptide library screened with recombinant GST-p75^NTR ICD revealed three distinct domains of PDE4A4 (asterisks in d) that interact with the ICD of p75^NTR: the LR1 domain (peptides 40 and 41), the catalytic domain (peptides 135 and 136) and the unique C terminus (peptides 172 and 173). (g) Alanine scanning mutagenesis shows that substitution of C862 abolishes the interaction of p75^NTR with the 173 peptide that is unique to PDE4A.
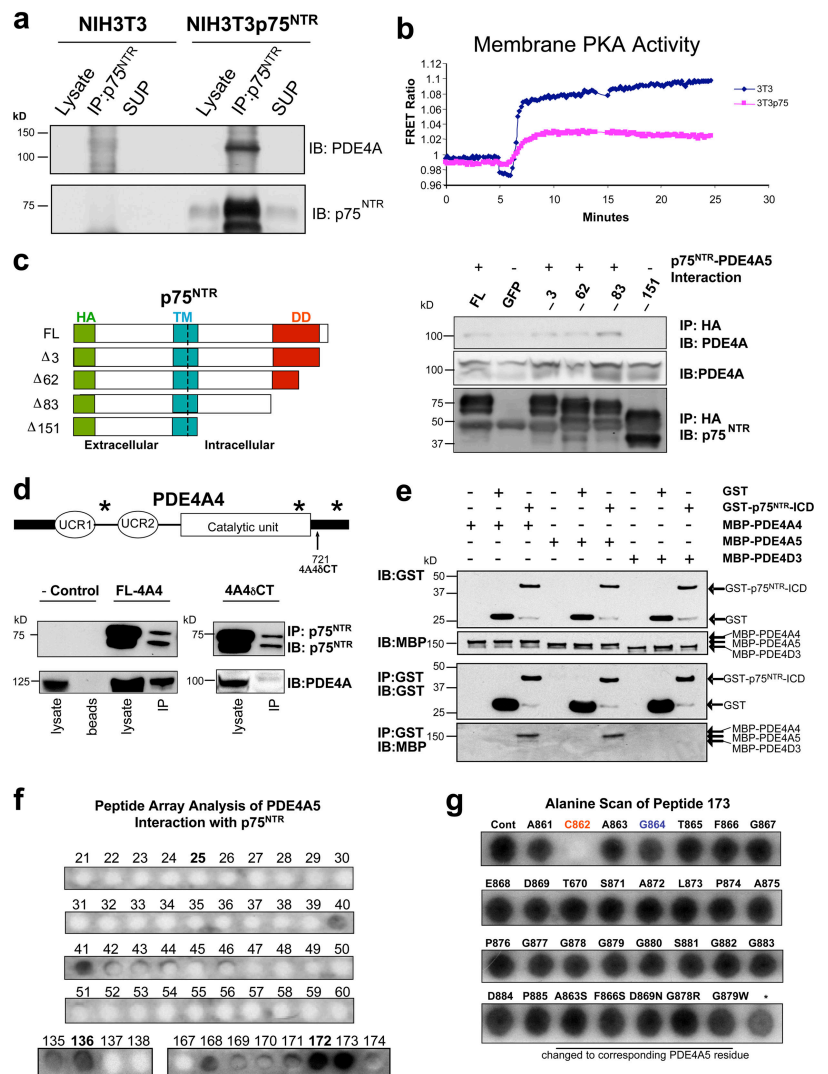
Δ83, but not a deletion missing the distal 151 amino acids, Δ151 (Fig. 8 c), suggesting that the interaction between p75^NTR and PDE4A5 occurs in the juxtamembrane region of p75^NTR, requiring sequences between residues 275 and 343. To explain the specificity of the interaction of p75^NTR with a single PDE4 isoform, we reasoned that p75^NTR would interact with a unique region of PDE4A5 that is not present in other PDE4s. Although the PDE4 isoforms are highly homologous, PDE4A5 contains a unique C-terminal region with a yet unknown biological function (Houslay and Adams, 2003). Co-IP experiments in HEK293 cells using the PDE4A4δCT mutant that is missing the C-terminal region (aa 721–886) abolishes the interaction with p75^NTR (Fig. 8 d).

To examine whether p75^NTR could interact with PDE4A5 in a direct manner, we performed in vitro pull-down assays using recombinant proteins. A GST fusion protein of p75^NTR encoding the entire ICD interacts with both recombinant PDE4A5 and its human homologue PDE4A4 (Fig. 8 e). In contrast, p75^NTR ICD does not interact with recombinant PDE4D3 (Fig. 8 e). These results are in accordance with both the endogenous co-IPs in cells (Fig. 8, a and c; Fig. S3) and the PDE4A4 mutagenesis data (Fig. 8 d) because similar to PDE4A4δCT, PDE4D3 does not contain the

unique C-terminal domain of PDE4A4/5. We have used peptide array technology to define sites of direct interaction in other PDE4s (Bolger et al., 2006). Screening a peptide array library of overlapping 25-mer peptides that scanned the sequence of PDE4A4 with GST-ICD p75^NTR identified interactions with the LR1 domain, whose sequence is unique to the PDE4A subfamily (peptides 40 and 41, aa 191–220), and also to a sequence within the catalytic domain (peptides 135 and 136, aa 671–700). However, the strongest interaction was observed with sequences within the C-terminal region of PDE4A4 (peptides 172 and 173, aa 856–885). Alanine scanning mutagenesis shows that substitution of C862 abolishes the interaction of p75^NTR with the 173 peptide that is unique to PDE4A (Fig. 8 g). The p75^NTR-interacting sequences within the LR1 and C-terminal domains are highly conserved between the human PDE4A4 and the rodent PDE4A5. Indeed, peptide array screening for PDE4A5 reveals direct interaction with p75^NTR similar to that seen for PDE4A4 (unpublished data). Overall, these results suggest that the interaction of p75^NTR with PDE4A4/5 is direct and that sequences within the juxtamembrane region of p75^NTR and the unique C-terminal region of PDE4A4/5 are primarily required for the interaction (Fig. 8, a, c–g; Fig. S3).
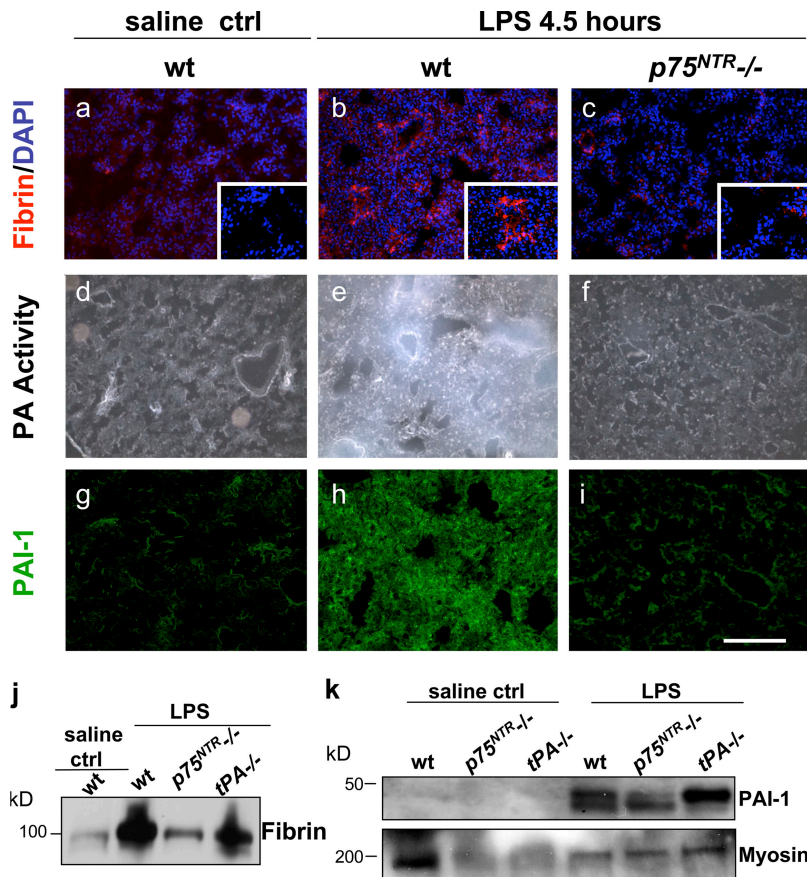
Figure 9. **p75^NTR regulates fibrin clearance in the lung.** LPS induces fibrin deposition (red) in the wt lung (b), when compared with the saline-injected lung (a). Lungs derived from *p75^NTR−/−* mice show less fibrin deposition (c). In situ zymography after 3 h of incubation shows clearance of casein in the lung of saline-injected wt (d), when compared with LPS injected wt lung (e). Lung from LPS-treated *p75^NTR−/−* mouse shows enhanced proteolytic activity (f), when compared with the wt mouse (e). Immunoreactivity for PAI-1 is increased in wt lung derived from LPS-treated mouse (h), when compared with saline-treated control (g). Lung from LPS-treated *p75^NTR−/−* mouse shows decreased PAI-1 (i), when compared with the wt LPS-treated mouse (h). (j) Western blot of fibrin precipitation from the lung shows an up-regulation of fibrin in the LPS-treated wt lung, when compared with the *p75^NTR−/−* lung. (k) Western blot for PAI-1 in the lung shows a decrease of PAI-1 in the *p75^NTR−/−* lung, when compared with the wt lung. Images are representative of n = 10 wt and n = 9 *p75^NTR−/−* mice. Western blots have been performed for n = 4 wt and n = 4 *p75^NTR−/−* mice. Bar: 150 μm (a–c), 75 μm (a–c, inset), 200 μm (d–f), 150 μm (g–i).

p75^NTR regulates plasminogen activation and fibrin deposition in a model of lipopolysaccharide-induced pulmonary fibrosis

Because expression of p75^NTR inhibits fibrinolysis in fibroblasts, we hypothesized that the role of p75^NTR as a modulator of fibrinolysis extends to tissues outside of the nervous system that express p75^NTR after injury or disease. Because p75^NTR is expressed in the lung (Ricci et al., 2004), we compared the levels of fibrin in the lung of wt and *p75^NTR−/−* mice in a model of lipopolysaccharide (LPS)-induced lung fibrosis (Chen et al., 2004). LPS-treated wt mice showed widespread extravascular fibrin deposition (Fig. 9 b) and decreased proteolytic activity after LPS treatment (Fig. 9 e), when compared with saline-treated wt mice (Fig. 9, a and d). In contrast, *p75^NTR−/−* mice show a 2.58-fold decrease of fibrin immunoreactivity (Fig. 9, c and j) and increased proteolytic activity (Fig. 9 f).

Decreased proteolytic activity in the lung after injury depends on the up-regulation of PAI-1 (Idell, 2003). Loss of PAI-1 protects from pulmonary fibrosis in LPS-induced airway disease, hyperoxia, and bleomycin-induced fibrosis (Savov et al., 2003). Because p75^NTR increases PAI-1 (Fig. 5 j and Fig. 6 e), we examined whether p75^NTR regulates expression of PAI-1 in vivo. PAI-1 is up-regulated in LPS-treated wt mice (Fig. 9 h) when compared with saline-treated wt mice (Fig. 9 g). In contrast, LPS-treated *p75^NTR−/−* mice show similar immunoreactivity for PAI-1 (Fig. 9 i) as saline-treated wt mice (Fig. 9 g), suggesting that p75^NTR induces up-regulation of PAI-1 after injury in the lung.

Western blots show a decrease in PAI-1 in the lungs of *p75^NTR−/−* mice (Fig. 9 k). Similar to the *p75^NTR−/−* mice, rolipram reduces fibrin deposition in the lung (Fig. S5, a and b; available at http://www.jcb.org/cgi/content/full/jcb.200701040/DC1) and sciatic nerve (Fig. S5, d–f), and decreases PAI-1 in the lung (Fig. S5 c), suggesting the involvement of PDE4 in p75^NTR-mediated inhibition of fibrinolysis in vivo. Collectively, our data show that p75^NTR increases fibrin deposition via a PDE4-mediated inhibition of plasminogen activation in both LPS-induced lung fibrosis and sciatic nerve crush injury. These data suggest a role for p75^NTR/PDE4 signaling as a general regulator of plasminogen activation and fibrinolysis at sites of injury.

Discussion

Our study shows a novel direct interaction of p75^NTR with PDE4A4/5, a specific PDE4 isoform, which results in the regulation of cAMP, a major intracellular signaling pathway, and mediates a major biological function of extracellular proteolysis and fibrinolysis (Fig. 10). p75^NTR is expressed in a wide range of tissue injury models, where repair depends upon both cell differentiation and ECM remodeling. For example, we recently showed that in the absence of plasminogen the effects of p75^NTR in tissue repair are protective due to its beneficial effects in cell differentiation (Passino et al., 2007). Similarly, in the flow-restricted carotid artery model of vascular injury that depends on uPA and not on tPA-mediated fibrinolysis (Kawasaki et al., 2001), p75^NTR is protective due to the induction of smooth

Figure 10. **Proposed model for the role of p75^NTR in the cAMP-mediated plasminogen activation.** p75^NTR interacts with PDE4A4/5 resulting in degradation of cAMP and thus a reduction of PKA activity. Decrease in cAMP reduces expression of tPA and increases PAI-1, resulting in reduction of plasmin and plasmin-dependent extracellular proteolysis. Reduction of plasmin results in reduced fibrin degradation and ECM remodeling. Because plasmin can proteolytically modify nonfibrin substrates, such as growth factors and cytokines, this mechanism may be upstream of various cellular functions.
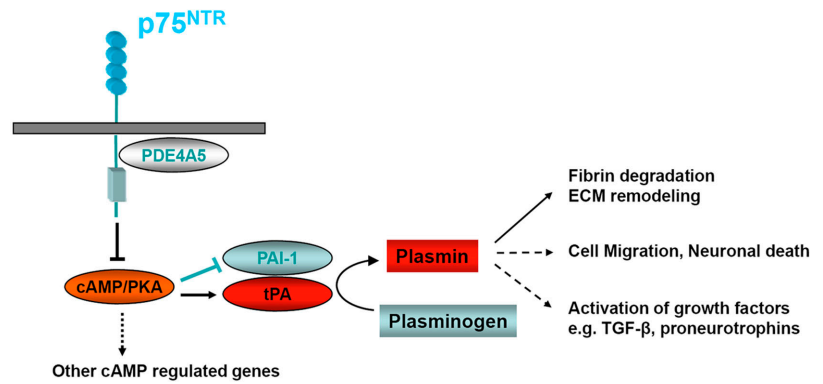
muscle cell apoptosis (Kraemer, 2002). In the sciatic nerve p75^NTR appears to have a dual role by sustaining fibrin deposition (our study), and also promoting myelination (Cosgaya et al., 2002; Song et al., 2006). Examination of functional recovery in $p75^{NTR-/-}$ mice after peripheral nerve injury would reveal the contribution of p75^NTR-mediated ECM remodeling and remyelination to the regeneration process. Overall, the biological role of p75^NTR after tissue injury would probably depend on the relative contributions of its role as a regulator of cell death and differentiation and its role as an inhibitor of fibrinolysis.

We identify regulation of cAMP as a novel signaling mechanism downstream of p75^NTR. Previous studies showed that β_2-adrenergic receptors target degradation of cAMP to the membrane via recruitment of multiple PDE4 isoforms, such as PDE4B1, PDE4B2, and PDE4Ds (Perry et al., 2002). Our finding of interaction between p75^NTR and PDE4A4/5 represents the first example of recruitment of a single PDE4 isoform to a transmembrane receptor. While interaction of β_2-adrenergic receptors with PDE4s is mediated via β-arrestin, our study suggests that the interaction of p75^NTR with PDE4A4/5 could be potentially mediated by direct binding to PDE4A domains, such as the C-terminal domain that is unique to this sub-family. In addition, in co-IP experiments we do not detect an interaction between p75^NTR and β-arrestin (unpublished data). It is possible that the unique C-terminal domain of PDE4A could regulate isoform-specific PDE4 recruitment to subcellular locations. Biological roles have been described for PDE4D in ischemic stroke (Gretarsdottir et al., 2003) and heart failure (Lehnart et al., 2005) and for PDE4B in schizophrenia (Millar et al., 2005). Our study identifies a biological function for PDE4A4/5 as a molecular mediator of p75^NTR/cAMP/PKA signaling involved in the regulation of tPA and fibrinolysis.

In spinal cord injury in rodents, elevation of cAMP via the PDE4 inhibitor, rolipram, promotes axonal regeneration and functional recovery (Nikulina et al., 2004). In the sciatic nerve, reduction of cAMP after injury is attributed primarily to up-regulation of PDE4 by SCs (Walikonis and Poduslo, 1998). Based on our findings, it is possible that reexpression of p75^NTR after injury could contribute to the activation of PDE4 and down-regulation of cAMP. BDNF, but not NGF, increases cAMP in neurons via TrkB (Gao et al., 2003). Moreover, BDNF/TrkB signaling overcomes the inhibition of nerve regeneration by myelin proteins via inhibition of PDE4 (Gao et al., 2003).

We provide the first evidence for p75^NTR in the regulation of cAMP by using genetic depletion, siRNA knockdown or up-regulation of the p75^NTR. Our results suggest that p75^NTR might exert the opposite function as Trk receptors by recruiting PDE4A4/5 and decreasing cAMP. Interestingly, PDE4A has been detected as the predominant PDE4 isoform at the corticospinal tract (Cherry and Davis, 1999). Because p75^NTR can act as a coreceptor for NogoR, a mediator of the inhibition of nerve regeneration, PDE4A interaction with p75^NTR could play an inhibitory role in nerve regeneration by competing with neurotrophin signaling via Trk receptors.

It is possible that the increased expression of p75^NTR by neurons, glia, and brain endothelial cells could regulate the temporal and spatial pattern of tPA expression during brain injury or inflammation. p75^NTR might also be upstream of other non-fibrinolytic functions associated with tPA, such as neurodegeneration, synaptic plasticity, and long-term potentiation (Samson and Medcalf, 2006). Given the dependence of p75^NTR functions on the availability of ligands and coreceptors (Teng and Hempstead, 2004; Reichardt, 2006), further analysis will determine the role of p75^NTR in extracellular proteolysis and ECM remodeling in different cellular systems. We show that expression of p75^NTR can inhibit tPA in the absence of neurotrophin ligands. Constitutive expression of p75^NTR may signal in a neurotrophin-independent manner to induce neuronal apoptosis (Rabizadeh et al., 1993), activation of Akt (Roux et al., 2001), and RhoGTPase (Yamashita et al., 1999). The regulation of cAMP identified here is an effect of expression of p75^NTR that does not appear to depend on neurotrophin signaling. The cellular distribution of PDE4A4/5 would determine the involvement of p75^NTR in the regulation of cAMP. It is possible that non-neurotrophin ligands that bind directly to p75^NTR, such as β-amyloid (Teng and Hempstead, 2004), as well as the myelin/NogoR p75^NTR–dependent inhibitors of nerve regeneration (Filbin, 2003), are able to regulate both cAMP and plasminogen activation by p75^NTR. Because cAMP analogues decrease expression of p75^NTR (Baron et al., 1997), it is possible that p75^NTR by decreasing cAMP contributes to the positive regulation of its expression. Because PKA phosphorylates p75^NTR and regulates its translocation to lipid rafts (Higuchi et al., 2003), p75^NTR via regulation of PKA might regulate its own subcellular localization. Given the multiple genes regulated by cAMP and PKA, other cellular functions may be regulated by p75^NTR/cAMP signaling.

NGF/p75^NTR signaling has been suggested to enhance local neurogenic inflammation to exacerbate pulmonary disease (Renz et al., 2004). Our study suggests an additional pathway for p75^NTR as a regulator of expression of PAI-1 and a mediator of fibrosis. p75^NTR in the lung is detected mainly in basal epithelial cells of bronchioles (unpublished data). Similar to p75^NTR, PAI-1 is expressed by bronchial epithelial cells (Savov et al., 2003) and its expression results in an antifibrinolytic environment within the airway wall. Fibrin regulates both inflammation and airway remodeling (Idell, 2003; Savov et al., 2003). It is therefore possible that p75^NTR-mediated regulation of PAI-1 via PDE4 could influence inflammatory and tissue repair processes in pulmonary disease. Although in chronic obstructive pulmonary disease the PDE4A4 isoform is specifically up-regulated (Barber et al., 2004) and considered a pharmacologic target (Houslay et al., 2005), all available inhibitors target the common catalytic domain of all PDE4 isoforms resulting in unwanted side-effects. Our study suggests that the p75^NTR/PDE4A4 interaction could be a potential therapeutic target that will achieve the specific inhibition of a single PDE4 isoform and may have therapeutic potential.

Collectively, we have identified a novel cAMP-dependent signaling pathway initiated by p75^NTR that specifically regulates plasminogen activity and scar formation after sciatic nerve and lung injury. Though p75^NTR is responsible for a variety of cell survival and death decisions (Chao, 2003), our data has revealed an unrecognized property of this receptor to regulate the degradation of cAMP. This property provides a potential mechanism to account for how p75^NTR acts at sites of injury to promote ECM remodeling. The impact of high levels of p75^NTR expression upon inhibition of extracellular proteolysis indicates that the detrimental effects of p75^NTR extend beyond cell growth and axon inhibition. Finally, the dramatic inhibitory effect of p75^NTR signaling on plasminogen activation suggests that the p75^NTR/PDE4A4 interaction represents a novel target for therapeutic intervention in both neuronal and non-neuronal tissues.

Materials and methods

Animals, sciatic nerve crush, and induction of lung fibrosis
p75^{NTR−/−} mice (Lee et al., 1992) and tPA^{−/−} mice (Carmeliet et al., 1994) were in C57Bl/6 background and purchased from The Jackson Laboratory. Double p75^{NTR−/−}tPA^{−/−} mice were generated by crossing p75^{NTR−/−} mice with tPA^{−/−} mice. C57Bl/6J mice were used as controls. Sciatic nerve crush was performed as described previously (Akassoglou et al., 2000). Lung fibrosis was induced as described previously (Chen et al., 2004). For the rolipram treatments, mice were administered 5 mg/kg rolipram (Calbiochem) before the LPS injection as described previously (Miotla et al., 1998). Mice were killed 4.5 h after LPS or saline administration. For rolipram treatment after sciatic nerve injury, mice were injected with rolipram (1 mg/kg) once daily for 8 d until tissue was harvested and processed for immunostaining.

Immunohistochemistry
Immunohistochemistry was performed as described in Akassoglou et al. (2002). Primary antibodies were sheep anti–human fibrin(ogen) (1:200; US Biologicals), rabbit anti–human tPA (1/300; Molecular Innovations), rabbit anti-p75^NTR clone 9651, (1:1,000), goat anti-p75^NTR (1/200; Santa Cruz Biotechnology, Inc.), rabbit anti–mouse PAI-1 (1:500; a gift from David Loskutoff, Scripps Research Institute, La Jolla, CA), and mouse anti-S100 (1:200; Neomarkers). For immunofluorescence, secondary antibodies

were anti–rabbit FITC and anti–goat Cy3 (1:200; Jackson Immunochemicals). Images were acquired with an Axioplan II epifluorescence microscope (Carl Zeiss MicroImaging, Inc.) using dry Plan-Neofluar lenses using 10× 0.3 NA, 20× 0.5 NA, or 40× 0.75 NA objectives equipped with Axiocam HRc digital camera and the Axiovision image analysis system.

Immunoblot
Immunoblot was performed as described previously (Akassoglou et al., 2002). Antibodies used were rabbit anti-p75^NTR clones 9992 and 9651 (1:5,000), mouse anti-fibrin (1:500; Accurate Chemical & Scientific Corp.), rabbit anti-myosin (1:1,000; Sigma-Aldrich), rabbit anti-GAPDH (1:5,000; Abcam) and rabbit anti-PAI-1 (1:5,000; a gift of David Loskutoff). Quantification was performed on the Scion NIH Imaging Software. Fibrin precipitation and quantification from lung tissues was performed exactly as described previously (Ling et al., 2004).

Co-IP
Co-IP was performed as described previously (Khursigara et al., 1999). Cell lysates were prepared in 1% NP-40, 200 mM NaCl, 1 mM EDTA, and 20 mM Tris-HCl, pH 8.0. IP was performed with an anti-p75^NTR antibody (9992) and immunoblot with anti-PDE4A, PDE4B, PDE4C, and PDE4D (Fabgennix). The co-IP buffer using NP-40 has been previously used to examine interactions of p75^NTR with other intracellular proteins, such as TRAF-6 (Khursigara et al., 1999) and PKA (Higuchi et al., 2003). For mapping experiments, PDE4A5 cDNA was cotransfected with HA-tagged p75^NTR deletion constructs into HEK293 cells. IP was performed with an anti-HA antibody (Cell Signaling). Cell lysates were probed with an anti-PDE4A or an anti-p75^NTR antibody (9651). For co-IP experiments using recombinant proteins, equimolar amounts (2 μM) of purified recombinant MBP-PDE4A5 (O'Connell et al., 1996), MPB-PDE4A4 (McPhee et al., 1999), MBP-PDE4D3 (Yarwood et al., 1999), and GST-p75^NTR-ICD (Khursigara et al., 2001) were mixed in binding buffer (50 mM Tris-HCl, pH 7.5, 100 mM NaCl, 2 mM MgCl$_2$, 1 mM DTT, 0.5% Triton X-100, and 0.5% BSA) and incubated for 1 h at 4°C. Washed glutathione-Sepharose beads were added according to the manufacturer's instructions for an additional hour. Beads were sedimented by centrifugation (10,000 g for 1 min) and washed three times. Proteins associated with the beads were eluted by boiling in loading buffer and separated by SDS-PAGE.

RT-PCR and real-time PCR
RT-PCR was performed as described previously (Akassoglou et al., 2002). Primers for tPA, uPA, and PAI-1 genes were used as described previously (Yamamoto and Loskutoff, 1996). Real-time PCR was performed using the Opticon DNA Engine 2 (MJ Research) and the Quantitect SYBR Green PCR kit (QIAGEN). Results were analyzed with Opticon 2 software using the comparative Ct method as described previously (Livak and Schmittgen, 2001). Data were expressed as ΔΔCt for the tPA gene normalized against GAPDH.

Quantification of tPA and uPA activity
Quantification of tPA and uPA activity in SC and fibroblast in lysates and supernatants was performed according to the directions of the activity assay kits from American Diagnostica and Chemicon, respectively. To elevate cAMP cells were treated either with 2 mM db-cAMP (Sigma-Aldrich) or with 10 μM forskolin (Sigma-Aldrich) for 16 h. To block PKA activity, cells were treated with 200 nM KT5720 (Calbiochem). Induction with neurotrophins was performed using 100 ng/ml NGF and 50 ng/ml BDNF for 16 h before tPA assay.

Fibrin degradation assay
Coating with fibrin was prepared as described previously (Lansink et al., 1998). To quantitate fibrin degradation, the supernatant was aspirated and the remaining gel was weighed using an analytical balance. Decrease of gel weight corresponded to increased fibrin gel degradation.

Cell culture and transfections
Murine SCs were isolated as described previously (Syroid et al., 2000). NIH3T3 or HEK293 cells were cotransfected either with p75^NTR FL, ICD or deletion constructs, and PDE4A5 cDNAs using Lipofectamine 2000 (Invitrogen) as described in the Results section. CGNs were isolated from P10 animals (Yamashita and Tohyama, 2003). CGNs were lysed immediately for co-IP, without plating. siRNA directed against p75^NTR (Dharmacon) was transfected into SCs and NIH3T3p75^NTR cells using Dharmafect (Dharmacon).

cAMP/PKA assays

10^6 fibroblasts or 500,000 SCs were lysed in 0.1 N HCl solution and cAMP was measured using a competitive binding cAMP ELISA (Assay Designs). Cells were treated with 100 ng/ml PTX for 16 h. For inhibition of PDE activity, cells were treated for 16 h with 500 μM isobutyl methylxanthine (IBMX; Calbiochem), 18.7 μM 8-methoxymethyl-3-isobutyl-1-methylxanthine (PDE1 inhibitor; Calbiochem), 80 μM *erythro*-9-(2-Hydroxy-3-nonyl)adenine (PDE2 inhibitor; Calbiochem), 100 nM trequinsin (PDE3 inhibitor; Calbiochem), and 10 μM rolipram (PDE4 inhibitor; Calbiochem). Cells were treated with forskolin in the presence of the inhibitors for 1 h. Because these inhibitors specifically inhibit a PDE isoform and have no effect on the other PDE isoenzymes (Beavo and Reifsnyder, 1990), they are extensively used for the identification of the specific PDE isoform that is involved in different cellular functions. Induction with neurotrophins was performed using 100 ng/ml NGF or 50 ng/ml BDNF, 750 ng/ml of FcTrkB, or 1.35 ug/ml of Fcp75[NTR] for 1 h before cAMP assay. For the qualitative and quantitative PKA assay (Promega), cells were treated with 10 μM forskolin for 30 min, lysed in 1% NP-40 buffer with 150 mM NaCl, 50 mM Tris, and 1 mM EGTA, and protein concentration was determined using the Bradford Assay (Bio- Rad Laboratories). 1 μg was loaded into the PKA assay reaction mix according to the manufacturer's protocol (Promega).

In situ zymography

In situ zymographies were performed as described previously (Akassoglou et al., 2000). Quantification of in situ zymographies was performed by measuring the area of the lytic zone surrounding each nerve, and dividing that value by the area of the nerve. Images were collected after 8 h of incubation for the sciatic nerve and 4 h of incubation for the lung. For cell zymographies, cultures were washed four times with PBS/BSA and overlaid with 200 μl of Dulbecco's minimum essential medium containing 1% LMP agarose, 2.5% boiled nonfat milk, and 25 μg/ml human plasminogen. The overlay was allowed to harden, and plates were incubated in a cell culture incubator at 37°C. Pictures of lytic zones were taken using an inverted microscope under dark field (Carl Zeiss MicroImaging, Inc.).

Construction of pm-AKAR2.2 and PDE4A4₈CT

For the construction of pm-AKAR2.2 we used the previously described cytoplasmic PKA sensor, AKAR2 (Zhang et al., 2005). pm-AKAR2.2 consists of a cDNA containing a FRET pair, monomeric enhanced cyan fluorescent protein (ECFP), and monomeric citrine (an optimized version of YFP), fused to forkhead associated domain 1 (FHA1) (Rad53p 22–162), and the PKA substrate sequence LRRATLVD via linkers. A206K mutations were incorporated to ECFP and Citrine by the QuikChange method (Stratagene). The C-terminal sequence from K-Ras KKKKKKSKTKCVIM was added to target the construct to the plasma membrane. For expression in mammalian cells, the chimaeric proteins were subcloned into a modified pcDNA3 vector (Invitrogen) behind a Kozak sequence as described previously (Zhang et al., 2005).

For the generation of the PDE4A4₈CT, PDE4A4 was subcloned into p3XFLAG-CMV-14 using plasmid pde46 (GenBank/EMBL/DDBJ accession no. L20965) as template from Met-1 to Iso-721 (McPhee et al., 1999). A forward (5′) primer containing a HindIII restriction site immediately 5′ to the initiating Met-1 (ATG) of PDE4A4 and a reverse primer designed to the DNA sequence ending at Iso-721 (ATA) with BamHI restriction site immediately 3′ to Iso-721 was used to amplify Met-1 to Iso-721. The C terminus was removed simply by amplifying from Iso-721 instead of the final codon at the end of the full-length PDE4A4B. The C-terminally truncated PDE4A4B was cloned in-frame with three FLAG (Asp-Tyr-Lys-Xaa-Xaa-Asp) epitopes (Asp-726, Asp-733 & Asp-740) after the BamHI restriction site, therefore at the C terminus of the now-truncated PDE4A4. The stop codon (TAG) after the FLAG epitopes is located immediately after Lys-747. This strategy generates a C-terminal truncate of PDE4A4 from 1–721.

FRET imaging

NIH3T3 cells and NIH3T3p75[NTR] cells were transiently transfected with pm-AKAR2.2, AKAR3, or pm-AKAR3 (Allen and Zhang, 2006) and imaged within 24 h of transfection. Cells were rinsed once with HBSS (Cellgro) before imaging in HBSS in the dark at room temperature. An Axiovert microscope (Carl Zeiss Microimaging, Inc.) with a MicroMax digital camera (Roper-Princeton Instruments) and MetaFluor software (Universal Imaging Corp.) was used to acquire all images. Optical filters were obtained from Chroma Technologies. CFP and FRET images were taken at 15-s intervals. Dual emission ratio imaging used a 420/20-nm excitation filter, a 450-nm dichroic mirror and a 475/40-nm or 535/25-nm emission filter for CFP and FRET, respectively. Excitation and emission filters were switched in filter wheels (Lambda 10–2; Sutter Instrument Co.).

Peptide array mapping

Peptide libraries were synthesized by automatic SPOT synthesis (Frank, 2002). Synthetic overlapping peptides (25 amino acids in length) were spotted on Whatman 50 cellulose membranes according to standard protocols by using Fmoc-chemistry with the AutoSpot Robot ASS 222 (Intavis Bioanalytical Instruments AG). Membranes were overlaid with 10 μg/ml recombinant GST-p75[NTR] ICD. Bound recombinant GST-p75[NTR] ICD (Khursigara et al., 2001) was detected using rabbit anti-GST (1:2,000; GE Healthcare) followed by secondary anti–rabbit horseradish peroxidase antibody (1:2,500; Dianova). Alanine scanning was performed as described previously (Bolger et al., 2006).

Statistics

Statistical significance was calculated using JMP2 Software by unpaired *t* test for isolated pairs or by analysis of variance (one-way ANOVA) for multiple comparisons. Data are shown as the mean ± SEM.

Online supplemental material

Fig. S1 shows that genetic loss of p75[NTR] increases tPA mRNA levels and proteolytic activity in the cerebellum. Fig. S2 demonstrates that treatment with neurotrophins has no effect on cAMP levels in NIH3T3 cells. Fig. S3 shows endogenous coimmunoprecipitations of PDE4A5 and p75[NTR] from injured sciatic nerve and from primary CGNs. Fig. S4 shows results from transient transfections of NIH3T3 cells with p75[NTR] and the PKA activity reporters, AKAR3 and pm-AKAR3. Fig. S5 shows that inhibition of PDE4s with rolipram decreases fibrin deposition both in LPS-induced lung fibrosis and sciatic nerve crush injury. The online version of this article is available at http://www.jcb.org/cgi/content/full/jcb.200701040/DC1.

References

Adams, R.A., M. Passino, B.D. Sachs, T. Nuriel, and K. Akassoglou. 2004. Fibrin mechanisms and functions in nervous system pathology. *Mol. Interv.* 4:163–176.

Akassoglou, K., K.W. Kombrinck, J.L. Degen, and S. Strickland. 2000. Tissue plasminogen activator-mediated fibrinolysis protects against axonal degeneration and demyelination after sciatic nerve injury. *J. Cell Biol.* 149:1157–1166.

Akassoglou, K., W.-M. Yu, P. Akpinar, and S. Strickland. 2002. Fibrin inhibits peripheral nerve regeneration by arresting Schwann cell differentiation. *Neuron.* 33:861–875.

Allen, M.D., and J. Zhang. 2006. Subcellular dynamics of protein kinase A activity visualized by FRET-based reporters. *Biochem. Biophys. Res. Commun.* 348:716–721.

Barber, R., G.S. Baillie, R. Bergmann, M.C. Shepherd, R. Sepper, M.D. Houslay, and G.V. Heeke. 2004. Differential expression of PDE4 cAMP phosphodiesterase isoforms in inflammatory cells of smokers with COPD, smokers without COPD, and nonsmokers. *Am. J. Physiol. Lung Cell. Mol. Physiol.* 287:L332–L343.

Baron, P., E. Scarpini, S. Pizzul, F. Zotti, G. Conti, D. Pleasure, and G. Scarlato. 1997. Immunocytochemical expression of human muscle cell p75 neurotrophin receptor is down-regulated by cyclic adenosine 3′,5′-monophosphate. *Neurosci. Lett.* 234:79–82.

Beattie, M.S., A.W. Harrington, R. Lee, J.Y. Kim, S.L. Boyce, F.M. Longo, J.C. Bresnahan, B.L. Hempstead, and S.O. Yoon. 2002. ProNGF induces p75-mediated death of oligodendrocytes following spinal cord injury. *Neuron.* 36:375–386.

Beavo, J.A., and D.H. Reifsnyder. 1990. Primary sequence of cyclic nucleotide phosphodiesterase isozymes and the design of selective inhibitors. *Trends Pharmacol. Sci.* 11:150–155.

Bolger, G.B., G.S. Baillie, X. Li, M.J. Lynch, P. Herzyk, A. Mohamed, L.H. Mitchell, A. McCahill, C. Hundsrucker, E. Klussmann, et al. 2006. Scanning peptide array analyses identify overlapping binding sites for the signalling scaffold proteins, beta-arrestin and RACK1, in cAMP-specific phosphodiesterase PDE4D5. *Biochem. J.* 398:23–36.

Brunton, L.L. 2003. PDE4: arrested at the border. *Sci. STKE.* 2003:PE44.

Bugge, T.H., K.W. Kombrinck, M.J. Flick, C.C. Daugherty, M.J. Danton, and J.L. Degen. 1996. Loss of fibrinogen rescues mice from the pleiotropic effects of plasminogen deficiency. *Cell.* 87:709–719.

Carmeliet, P., L. Schoonjans, L. Kieckens, B. Ream, J. Degen, R. Bronson, R. De Vos, J.J. van den Oord, D. Collen, and R.C. Mulligan. 1994. Physiological consequences of loss of plasminogen activator gene function in mice. *Nature.* 368:419–424.

Chao, M.V. 2003. Neurotrophins and their receptors: a convergence point for many signalling pathways. *Nat. Rev. Neurosci.* 4:299–309.

Chen, D., K. Giannopoulos, P.G. Shiels, Z. Webster, J.H. McVey, G. Kemball-Cook, E. Tuddenham, M. Moore, R. Lechler, and A. Dorling. 2004. Inhibition of intravascular thrombosis in murine endotoxemia by targeted expression of hirudin and tissue factor pathway inhibitor analogs to activated endothelium. *Blood.* 104:1344–1349.

Cherry, J.A., and R.L. Davis. 1999. Cyclic AMP phosphodiesterases are localized in regions of the mouse brain associated with reinforcement, movement, and affect. *J. Comp. Neurol.* 407:287–301.

Cosgaya, J.M., J.R. Chan, and E.M. Shooter. 2002. The neurotrophin receptor p75NTR as a positive modulator of myelination. *Science.* 298:1245–1248.

Degen, J.L., A.F. Drew, J.S. Palumbo, K.W. Kombrinck, J.A. Bezerra, M.J. Danton, K. Holmback, and T.T. Suh. 2001. Genetic manipulation of fibrinogen and fibrinolysis in mice. *Ann. N. Y. Acad. Sci.* 936:276–290.

Dowling, P., X. Ming, S. Raval, W. Husar, P. Casaccia-Bonnefil, M. Chao, S. Cook, and B. Blumberg. 1999. Up-regulated p75NTR neurotrophin receptor on glial cells in MS plaques. *Neurology.* 53:1676–1682.

Filbin, M.T. 2003. Myelin-associated inhibitors of axonal regeneration in the adult mammalian CNS. *Nat. Rev. Neurosci.* 4:703–713.

Fiumelli, H., D. Jabaudon, P.J. Magistretti, and J.-L. Martin. 1999. BDNF stimulates expression, activity and release of tissue-type plasminogen activator in mouse cortical neurons. *Eur. J. Neurosci.* 11:1639–1646.

Frank, R. 2002. The SPOT-synthesis technique. Synthetic peptide arrays on membrane supports–principles and applications. *J. Immunol. Methods.* 267:13–26.

Gao, Y., E. Nikulina, W. Mellado, and M.T. Filbin. 2003. Neurotrophins elevate cAMP to reach a threshold required to overcome inhibition by MAG through extracellular signal-regulated kinase-dependent inhibition of phosphodiesterase. *J. Neurosci.* 23:11770–11777.

Gretarsdottir, S., G. Thorleifsson, S.T. Reynisdottir, A. Manolescu, S. Jonsdottir, T. Jonsdottir, T. Gudmundsdottir, S.M. Bjarnadottir, O.B. Einarsson, H.M. Gudjonsdottir, et al. 2003. The gene encoding phosphodiesterase 4D confers risk of ischemic stroke. *Nat. Genet.* 35:131–138.

Herrmann, J.L., D.G. Menter, J. Hamada, D. Marchetti, M. Nakajima, and G.L. Nicolson. 1993. Mediation of NGF-stimulated extracellular matrix invasion by the human melanoma low-affinity p75 neurotrophin receptor: melanoma p75 functions independently of trkA. *Mol. Biol. Cell.* 4:1205–1216.

Higuchi, H., T. Yamashita, H. Yoshikawa, and M. Tohyama. 2003. PKA phosphorylates the p75 receptor and regulates its localization to lipid rafts. *EMBO J.* 22:1790–1800.

Houslay, M.D., and D.R. Adams. 2003. PDE4 cAMP phosphodiesterases: modular enzymes that orchestrate signalling cross-talk, desensitization and compartmentalization. *Biochem. J.* 370:1–18.

Houslay, M.D., P. Schafer, and K.Y. Zhang. 2005. Keynote review: phosphodiesterase-4 as a therapeutic target. *Drug Discov. Today.* 10:1503–1519.

Hsu, K.C., and M.V. Chao. 1993. Differential expression and ligand binding properties of tumor necrosis factor receptor chimeric mutants. *J. Biol. Chem.* 268:16430–16436.

Idell, S. 2003. Coagulation, fibrinolysis, and fibrin deposition in acute lung injury. *Crit. Care Med.* 31:S213–S220.

Kawasaki, T., M. Dewerchin, H.R. Lijnen, I. Vreys, J. Vermylen, and M.F. Hoylaerts. 2001. Mouse carotid artery ligation induces platelet-leukocyte-dependent luminal fibrin, required for neointima development. *Circ. Res.* 88:159–166.

Khursigara, G., J.R. Orlinick, and M.V. Chao. 1999. Association of the p75 neurotrophin receptor with TRAF6. *J. Biol. Chem.* 274:2597–2600.

Khursigara, G., J. Bertin, H. Yano, H. Moffett, P.S. DiStefano, and M.V. Chao. 2001. A prosurvival function for the p75 receptor death domain mediated via the caspase recruitment domain receptor-interacting protein 2. *J. Neurosci.* 21:5854–5863.

Kraemer, R. 2002. Reduced apoptosis and increased lesion development in the flow-restricted carotid artery of p75(NTR)-null mutant mice. *Circ. Res.* 91:494–500.

Lansink, M., P. Koolwijk, V. van Hinsbergh, and T. Kooistra. 1998. Effect of steroid hormones and retinoids on the formation of capillary-like tubular structures of human microvascular endothelial cells in fibrin matrices is related to urokinase expression. *Blood.* 92:927–938.

Lee, K.F., E. Li, L.J. Huber, S.C. Landis, A.H. Sharpe, M.V. Chao, and R. Jaenisch. 1992. Targeted mutation of the gene encoding the low affinity NGF receptor p75 leads to deficits in the peripheral sensory nervous system. *Cell.* 69:737–749.

Lee, R., P. Kermani, K.K. Teng, and B.L. Hempstead. 2001. Regulation of cell survival by secreted proneurotrophins. *Science.* 294:1945–1948.

Lehnart, S.E., X.H. Wehrens, S. Reiken, S. Warrier, A.E. Belevych, R.D. Harvey, W. Richter, S.L. Jin, M. Conti, and A.R. Marks. 2005. Phosphodiesterase 4D deficiency in the ryanodine-receptor complex promotes heart failure and arrhythmias. *Cell.* 123:25–35.

Lemke, G., and M. Chao. 1988. Axons regulate Schwann cell expression of the major myelin and NGF receptor genes. *Development.* 102:499–504.

Lijnen, H.R. 2001. Elements of the fibrinolytic system. *Ann. N. Y. Acad. Sci.* 936:226–236.

Ling, Q., A.T. Jacovina, A. Deora, M. Febbraio, R. Simantov, R.L. Silverstein, B. Hempstead, W.H. Mark, and K.A. Hajjar. 2004. Annexin II regulates fibrin homeostasis and neoangiogenesis in vivo. *J. Clin. Invest.* 113:38–48.

Livak, K.J., and T.D. Schmittgen. 2001. Analysis of relative gene expression data using real-time quantitative PCR and the 2(-Delta Delta C(T)) method. *Methods.* 25:402–408.

Lomen-Hoerth, C., and E.M. Shooter. 1995. Widespread neurotrophin receptor expression in the immune system and other nonneuronal rat tissues. *J. Neurochem.* 64:1780–1789.

McPhee, I., S.J. Yarwood, G. Scotland, E. Huston, M.B. Beard, A.H. Ross, E.S. Houslay, and M.D. Houslay. 1999. Association with the SRC family tyrosyl kinase LYN triggers a conformational change in the catalytic region of human cAMP-specific phosphodiesterase HSPDE4A4B. Consequences for rolipram inhibition. *J. Biol. Chem.* 274:11796–11810.

Medcalf, R.L., M. Ruegg, and W.D. Schleuning. 1990. A DNA motif related to the cAMP-responsive element and an exon-located activator protein-2 binding site in the human tissue-type plasminogen activator gene promoter cooperate in basal expression and convey activation by phorbol ester and cAMP. *J. Biol. Chem.* 265:14618–14626.

Millar, J.K., B.S. Pickard, S. Mackie, R. James, S. Christie, S.R. Buchanan, M.P. Malloy, J.E. Chubb, E. Huston, G.S. Baillie, et al. 2005. DISC1 and PDE4B are interacting genetic factors in schizophrenia that regulate cAMP signaling. *Science.* 310:1187–1191.

Miotla, J.M., M.M. Teixeira, and P.G. Hellewell. 1998. Suppression of acute lung injury in mice by an inhibitor of phosphodiesterase type 4. *Am. J. Respir. Cell Mol. Biol.* 18:411–420.

Nikulina, E., J.L. Tidwell, H.N. Dai, B.S. Bregman, and M.T. Filbin. 2004. The phosphodiesterase inhibitor rolipram delivered after a spinal cord lesion promotes axonal regeneration and functional recovery. *Proc. Natl. Acad. Sci. USA.* 101:8786–8790.

O'Connell, J.C., J.F. McCallum, I. McPhee, J. Wakefield, E.S. Houslay, W. Wishart, G. Bolger, M. Frame, and M.D. Houslay. 1996. The SH3 domain of Src tyrosyl protein kinase interacts with the N-terminal splice region of the PDE4A cAMP-specific phosphodiesterase RPDE-6 (RNPDE4A5). *Biochem. J.* 318(Pt 1):255–261.

Park, J.A., J.Y. Lee, T.A. Sato, and J.Y. Koh. 2000. Co-induction of p75NTR and p75NTR-associated death executor in neurons after zinc exposure in cortical culture or transient ischemia in the rat. *J. Neurosci.* 20:9096–9103.

Passino, M.A., R.A. Adams, S.L. Sikorski, and K. Akassoglou. 2007. Regulation of hepatic stellate cell differentiation by the neurotrophin receptor p75NTR. *Science.* 315:1853–1856.

Perry, S.J., G.S. Baillie, T.A. Kohout, I. McPhee, M.M. Magiera, K.L. Ang, W.E. Miller, A.J. McLean, M. Conti, M.D. Houslay, and R.J. Lefkowitz. 2002. Targeting of cyclic AMP degradation to beta 2-adrenergic receptors by beta-arrestins. *Science.* 298:834–836.

Qian, Z., M.E. Gilbert, M.A. Colicos, E.R. Kandel, and D. Kuhl. 1993. Tissue-plasminogen activator is induced as an immediate-early gene during seizure, kindling and long-term potentiation. *Nature.* 361:453–457.

Rabizadeh, S., J. Oh, L.T. Zhong, J. Yang, C.M. Bitler, L.L. Butcher, and D.E. Bredesen. 1993. Induction of apoptosis by the low-affinity NGF receptor. *Science.* 261:345–348.

Reichardt, L.F. 2006. Neurotrophin-regulated signalling pathways. *Philos. Trans. R. Soc. Lond. B Biol. Sci.* 361:1545–1564.

Renz, H., S. Kerzel, and W.A. Nockher. 2004. The role of neurotrophins in bronchial asthma: contribution of the pan-neurotrophin receptor p75. *Prog. Brain Res.* 146:325–333.

Ricci, A., L. Felici, S. Mariotta, F. Mannino, G. Schmid, C. Terzano, G. Cardillo, F. Amenta, and E. Bronzetti. 2004. Neurotrophin and neurotrophin receptor protein expression in the human lung. *Am. J. Respir. Cell Mol. Biol.* 30:12–19.

Roux, P.P., A.L. Bhakar, T.E. Kennedy, and P.A. Barker. 2001. The p75 neurotrophin receptor activates Akt (protein kinase B) through a phosphatidylinositol 3-kinase-dependent pathway. *J. Biol. Chem.* 276:23097–23104.

Samson, A.L., and R.L. Medcalf. 2006. Tissue-type plasminogen activator: a multifaceted modulator of neurotransmission and synaptic plasticity. *Neuron.* 50:673–678.

Santell, L., and E. Levin. 1988. Cyclic AMP potentiates phorbol ester stimulation of tissue plasminogen activator release and inhibits secretion of plasminogen activator inhibitor-1 from human endothelial cells. *J. Biol. Chem.* 263:16802–16808.

Savov, J.D., D.M. Brass, K.G. Berman, E. McElvania, and D.A. Schwartz. 2003. Fibrinolysis in LPS-induced chronic airway disease. *Am. J. Physiol. Lung Cell. Mol. Physiol.* 285:L940–L948.

Siconolfi, L.B., and N.W. Seeds. 2001. Mice lacking tPA, uPA, or plasminogen genes showed delayed functional recovery after sciatic nerve crush. *J. Neurosci.* 21:4348–4355.

Song, X.Y., F.H. Zhou, J.H. Zhong, L.L. Wu, and X.F. Zhou. 2006. Knockout of p75(NTR) impairs re-myelination of injured sciatic nerve in mice. *J. Neurochem.* 96:833–842.

Syroid, D.E., P.J. Maycox, M. Soilu-Hanninen, S. Petratos, T. Bucci, P. Burrola, S. Murray, S. Cheema, K.F. Lee, G. Lemke, and T.J. Kilpatrick. 2000. Induction of postnatal Schwann cell death by the low-affinity neurotrophin receptor in vitro and after axotomy. *J. Neurosci.* 20:5741–5747.

Taniuchi, M., H.B. Clark, and E.M. Johnson Jr. 1986. Induction of nerve growth factor receptor in Schwann cells after axotomy. *Proc. Natl. Acad. Sci. USA.* 83:4094–4098.

Teng, K.K., and B.L. Hempstead. 2004. Neurotrophins and their receptors: signaling trios in complex biological systems. *Cell. Mol. Life Sci.* 61:35–48.

Walikonis, R.S., and J.F. Poduslo. 1998. Activity of cyclic AMP phosphodiesterases and adenylyl cyclase in peripheral nerve after crush and permanent transection injuries. *J. Biol. Chem.* 273:9070–9077.

Wang, S., P. Bray, T. McCaffrey, K. March, B.L. Hempstead, and R. Kraemer. 2000. p75(NTR) mediates neurotrophin-induced apoptosis of vascular smooth muscle cells. *Am. J. Pathol.* 157:1247–1258.

Yamamoto, K., and D.J. Loskutoff. 1996. Fibrin deposition in tissues from endotoxin-treated mice correlates with decreases in the expression of urokinase-type but not tissue-type plasminogen activator. *J. Clin. Invest.* 97:2440–2451.

Yamashita, T., and M. Tohyama. 2003. The p75 receptor acts as a displacement factor that releases Rho from Rho-GDI. *Nat. Neurosci.* 6:461–467.

Yamashita, T., K.L. Tucker, and Y.A. Barde. 1999. Neurotrophin binding to the p75 receptor modulates Rho activity and axonal outgrowth. *Neuron.* 24:585–593.

Yarwood, S.J., M.R. Steele, G. Scotland, M.D. Houslay, and G.B. Bolger. 1999. The RACK1 signaling scaffold protein selectively interacts with the cAMP-specific phosphodiesterase PDE4D5 isoform. *J. Biol. Chem.* 274:14909–14917.

Zhang, J., C.J. Hupfeld, S.S. Taylor, J.M. Olefsky, and R.Y. Tsien. 2005. Insulin disrupts beta-adrenergic signalling to protein kinase A in adipocytes. *Nature.* 437:569–573.

Zorick, T.S., and G. Lemke. 1996. Schwann cell differentiation. *Curr. Opin. Cell Biol.* 8:870–876.